SPECTROSCOPIC SIGNATURES OF MICROJETS

J. SOLF
Thüringer Landessternwarte Tautenburg,
Sternwarte 5, D-77778 Tautenburg, FRG

Abstract. High-resolution long-slit spectroscopy of forbidden emission lines is used to investigate on a sub-arcsecond scale the spatial and kinematic properties and the physical conditions of the mass outflows from T Tauri stars in the immediate vicinity of the outflow source (microjets). Special attention is given to the case of DG Tau. The data permit us to distinguish physically different outflow components: (1) a high-velocity component (HVC) attributed to a fast jet, (2) a low-velocity component (LVC) attributed to gas entrained by the jet, and (3) a near-rest-velocity component (NRVC) attributed to a slow disk wind and/or disk corona.

1. Introduction

Forbidden emission lines (FELs) observed in the mass outflows from young stellar objects can be used as powerful diagnostic probes to study the morphology and kinematics as well as the physical conditions of the various manifestations of outflows, such as (bipolar) jets or Herbig-Haro (HH) objects. At optical wavelengths the spectra of the outflows are dominated by the lines of [OI], [NII] and [SII], indicating shocks as the main source of excitation in the outflowing gas. Classical T Tauri stars (TTSs) exhibit FELs superimposed upon the photospheric continuum spectrum. Since these lines are observed near the stellar position, their analysis has provided useful information on the properties of the outflows in the vicinity of their (stellar) outflow source (Appenzeller, Jankovics and Östreicher 1984; Edwards et al. 1987; Hamann 1994; Hartigan, Edwards & Ghandour 1995).

FELs observed in TTSs are more often blueshifted (with respect to the stellar velocity). This has been explained as due to a bipolar outflow of which the (redshifted) receding portion is hidden by an opaque circumstellar disk. Double-peaked FEL profiles are quite common consisting of a

B. Reipurth and C. Bertout (eds.), Herbig–Haro Flows and the Birth of Low Mass Stars, 63–72.

"low-velocity component" (LVC) and a "high-velocity component" (HVC). Several attempts have been made to understand the nature of the LVC and HVC. In most cases, a single outflow component has been assumed and it has been tried to interpret the double-peaked line profiles as due to geometric projection effects (e.g. Edwards et al. 1987; Hartmann & Raymond 1989; Gómez de Castro & Pudritz 1993; Ouyed & Pudritz 1993). In contrast, Kwan & Tademaru (1988; 1995) have noted that the [OI] line characteristics derived for the LVC and HVC are not readily explained by a single outflow component and proposed the existence of two physically distinct gas components in the outflows. According to their model the HVC is attributed to a high-speed gas in a jet-like flow due to a stellar wind that is collimated by the magnetic field in the circumstellar disk, whereas the LVC is attributed to an intrinsically low-speed gas due to a wind from the circumstellar disk and/or a disk corona.

As shown in previous work (Solf 1989), high-resolution long-slit spectroscopy of the FELs in TTSs can provide detailed information on a subarcsecond scale about both the spatial and the kinematic properties of the various outflow components in the immediate vicinity of the outflow source. Since in many cases the length of the outflow features observed in the vicinity of the star is quite small (less than a few arcseconds) these outflows have been nicknamed "microjets". Several long-slit spectroscopic studies of the FELs in TTSs (Solf & Böhm 1993; Böhm & Solf 1994; Hirth, Mundt & Solf 1994a, 1997; Hirth et al. 1994b) have been carried out in order to investigate the spatial and spectral properties of the microjets. The results of these studies support the interpretation of the HVC and LVC according to the Kwan & Tademaru model.

In this contribution, after a brief account on the applied observational and data reduction techniques, I will summarize the general characteristics of the spectroscopic signatures of microjets. Special attention will be given to the case of DG Tau which may be considered as a prototype for these outflows and for which more detailed observations from a period of serveral years are available.

2. Observations and Data Reduction Techniques

Using the Coudé spectrograph of the 2.2-m telescope at the Calar Alto Observatory (Spain), for each object several long-slit spectra have been obtained with the entrance slit centered on the star and oriented at various position angles (PA), preferentially parallel and perpendicular to the main outflow direction. A typical spectral resolution (FWHM) of $\sim$10 km s^{-1} and a spatial resolution (FWHM) of $0.''7 - 1.''5$ along the slit direction have been achieved. From each spectrogram a position velocity (PV) diagram of

the (spatially and spectrally resolved) FEL regions covered by the slit has been deduced. A more detailed description of the observational and data reduction techniques has been given elsewhere (Solf 1989; 1994).

Perhaps the most important aspect in the data reduction and analysis of the FELs on long-slit spectrograms of TTSs comes from the presence of the underlying stellar continuum on the same spectrogram. *Firstly,* the continuum in the spectral range of the FELs has to be removed. This can be done effectively by evaluating the actual amount to be subtracted from an interpolation of the heights of the continuum on either side of the FEL. In order to account for absorption lines in the stellar spectrum underneath (and hidden by) the FEL, a template stellar spectrum (with similar absorption line characteristics but without the FEL) is used in the subtraction procedure. *Secondly,* the spatial distribution of the continuum (along the slit direction) can be used to determine accurately both the stellar position and the actual spatial resolution (FWHM). This permits us to evaluate with high accuracy (1) the position of the centroid of each FEL component relative to the stellar position and (2) its spatial extent (FWHM) corrected for the actual resolution. The strictly differential method permits us to measure the position of FEL components with an accuracy of $\sim 0.''02$ and to determine their spatial extent (corrected FWHM) down to $\sim 0.''2$.

3. Results and Discussion

3.1. SPECTROSCOPIC SIGNATURES OF MICROJETS

As already noted, the FELs observed in TTSs are more often blueshifted. If redshifted FEL features are present as well, these are usually fainter than the blueshifted ones. In many cases, the FEL profiles are rather complex presenting, e. g., double peaks, although single-peaked profiles occur quite often. In the latter case, the emission peak is usually quite narrow and only slightly blueshifted, typically at -5 km s^{-1} (Hamann 1994; Hartigan et al. 1995). This "near-rest-velocity component" (NRVC) is sometimes present in the more complex FEL profiles as well and sometimes confused by other line components. As noted by Hamann (1994), the NRVC has to be distinguished from the LVC (peaking at $\leq \pm 50$ km s^{-1}), since these two components may represent distinct emitting gas regions. In some cases, the HVC (usually observed at $\geq \pm 100$ km s^{-1}) is not well separated from the LVC in a particular FEL. In these cases, the distinction between the various components is based on their relative strengths in different FELs (e. g. [NII] and [SII]). The deduced spatio-kinematic properties provide additional criteria for distinguishing the various FEL components.

Although there may be many particularities varying from object to object, the more general characteristics of the spatial and kinematic properties

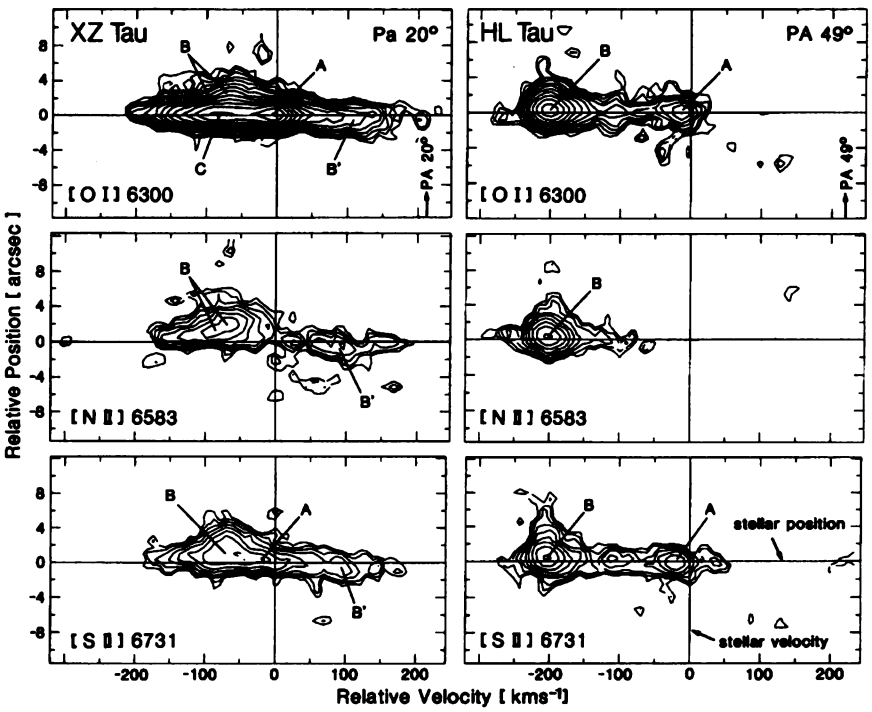

Figure 1. PV diagrams of the [OI]λ6300, [NII]λ6583 and [SII]λ6731 lines in XZ Tau and HL Tau derived from long-slit spectrograms obtained with the slit parallel to the outflow directions. The stellar continuum has been removed. Contours represent a factor of $2^{1/2}$ in the intensity. Velocities and positions are quoted with respect to the stellar velocity and stellar position, respectively.

of the outflows in the vicinity of the outflow source (microjets) are well illustrated by the observations of the FEL regions in XZ Tau and HL Tau. Fig. 1 shows the PV diagrams of the lines of [OI]λ6300, [NII]λ6583, and [SII]λ6731 obtained with the slit parallel to the bipolar outflow directions. XZ Tau presents both blueshifted and (fainter) redshifted FEL features located on opposite sides with respect to the central star as expected for a bipolar outflow of which the receding portion is partially obscured by a circumstellar disk. As can be noted on Fig. 1, in both stars the HVC (marked B) is present in all lines observed, whereas the LVC (marked A) is not present in [NII]. Compared to the LVC, the HVC is broader in velocity, spatially more extended along the outflow direction, and its centroid is separated from the star by a larger offset. Although the overall extent of the HVC is comparable in all three lines, the [OI]λ6300 emission is much

https://doi.org/10.1017/S0074180900061544 Published online by Cambridge University Press

more concentrated close to the central star. Nevertheless, the [OI] emission centroid of the HVC (marked C in the case of XZ Tau) is still clearly offset from the stellar position.

In a long-slit spectroscopic survey of 38 TTSs Hirth, Mundt & Solf (1997) have studied the spatial and kinematic properties of the FEL regions of [OI]$\lambda\lambda$6300,6363, [NII]$\lambda\lambda$6548,6583, and [SII]$\lambda\lambda$6716,6731 and derived the following main results: Generally, the HVC is spatially more extended than the LVC. In the [SII] lines, the emission centroid of the HVC is separated from the stellar position by a typical offset of $0.''6$; the typical offset of the LVC is more than a factor 3 smaller. In the [NII] lines, detected in the HVC only, both the spatial extent and offset from the star are usually somewhat larger compared to the other FELs observed. In the [OI] lines, the offset of the emission centroid of the HVC is much smaller than in the other lines (typically $\sim 0.''2$). The LVC generally presents the highest compactness and the smallest offset of its emission centroid from the star (typically $\sim 0.''1$ in [OI] and $\sim 0.''2$ in [SII]).

3.2. THE CASE OF DG TAU

3.2.1. *General remarks*

DG Tau is a source of collimated mass outflows observed in (blueshifted) FEL condensations extending up to $\sim 10''$ towards PA 225° (Mundt & Fried 1983; Mundt, Brugel & Bührke 1987). On direct images of DG Tau in the light of FELs (see, e.g., Solf & Böhm 1993), one can recognize an inner region of the outflow (up to $\sim 4''$ from the star), containing the "microjet", and an outer region (from $\sim 5''$ to $\sim 10''$), containing several HH condensations. Adopting a distance of 140 pc, an inclination angle (with respect to the plane of the sky) of $\sim 51°$ has been deduced for the outflow direction using the proper motions and radial velocities derived for the HH condensations (Eislöffel 1992).

On direct images of DG Tau, the microjet region is heavily confused by the presence of the much stronger stellar continuum. On long-slit spectrograms of DG Tau, however, the underlying continuum spectrum can be effectively removed. Fig. 2 presents PV diagrams of the lines of [SII]λ6731, [NII]λ6583, [OI]λ6300, and[OI]λ5577 deduced from long-slit spectrograms obtained with the slit parallel to the outflow direction (PA 45°). The PV diagrams permit us to distinguish various line features (designated A, A', B and C) on the basis of their kinematic and spatial characteristics.

Features B and C show both high velocities. B appears in the lines of [SII]λ6731, [NII]λ6583, and [OI]λ6300, whereas C is present in [OI]λ6300 only (and marginally detected in [OI]λ5577). B is spatially more extended than C. As already pointed out by Solf & Böhm (1993), both the (mean)

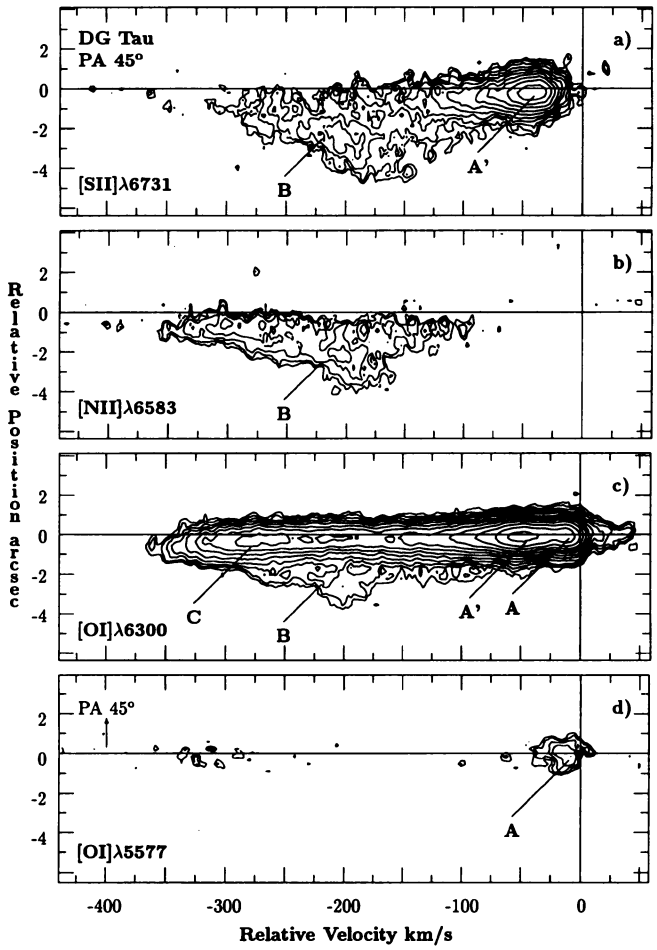

Figure 2. PV diagrams of the line emission of [SII]λ6731, [NII]λ6583, [OI]λ6300, and [OI]λ5577 in DG Tau. The diagrams have been deduced from PA 45° long-slit spectrograms obtained in 1992 (slit parallel to the outflow direction). Contours, velocities and positions as in Fig. 1

velocity and the electron density deduced within feature B are strongly increasing with decreasing distance from the central star and that trend continues within feature C. Therefore, B and C, rather than representing two separate outflow components, are considered to trace the outer (lower-density) and the inner (higher-density) regions, respectively, of one and the same "high-velocity" gas component (HVC).

Features A and A' show both low velocities. The velocity of A, lower than that of A', is near the (stellar) rest velocity. Both features are present

https://doi.org/10.1017/S0074180900061544 Published online by Cambridge University Press

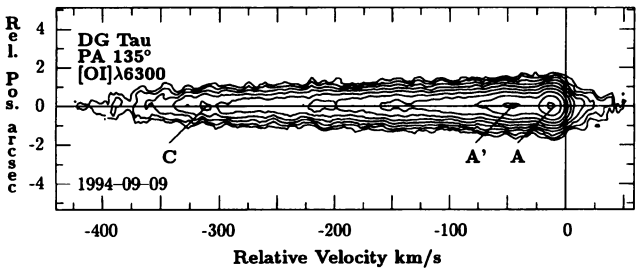

Figure 3. PV diagram of the [OI]λ6300 line in DG Tau at PA 135° (slit perpendicular to the outflow direction). Contours, velocities and position as in Fig. 1

in [OI]λ6300 and both absent in [NII]λ6583. The distinction between A and A' as two separate components is based on the fact that A is observed in [OI]λ6300 and [OI]λ5577, but not observed in [SII]λ6731, whereas A' is observed in [SII]λ6731 and [OI]λ6300, but not observed in [OI]λ5577. These findings indicate that the electron density is much higher in A ($\geq 10^7$ cm^{-3}) than in A' ($\geq 10^5$ cm^{-3}). Adopting the denominations proposed by Hamann (1994) we attribute feature A' to a "low-velocity" gas component (LVC), and feature A to a "near-rest-velocity" gas component (NRVC).

3.2.2. *Time variability*

The destinction between A and A' as two separate gas components in the outflows is strongly supported by a time series (from 1992 to 1994) of observations of DG Tau. As can be noted on the PV diagrams of the [OI]λ6300 line (Fig. 4) and the corresponding intensity profiles (Fig. 5), the relative line strengths of A and A' exhibit dramatic changes during that time period. Feature A, much weaker than A' in 1992, became the dominant feature in 1994. Furthermore, the time series reveals remarkable changes in the HVC as well. The "terminal" velocity ("blue edge") of feature C increased from ~ -350 km s^{-1} in 1992 to ~ -420 km s^{-1} in 1994.

3.2.3. *The high-velocity gas component (HVC)*

As already pointed out, the HVC is attributed to the high-speed gas of a jet-like outflow. Features B and C (see Figs. 2, 4) represent the outer and inner regions of the microjet, respectively. The relatively narrow outer tip of B (at $\sim 4''$ offset) shows a velocity of about -200 km s^{-1}, only slightly larger than that of the more distant HH condensations (-160 km s^{-1}). Both the mean velocity and velocity width deduced for the jet flow increase towards the central star. Similarily, an increase of the electron density in the jet of up to $>10^4$ cm^{-3} has been deduced from the [SII] line ratio. Due to

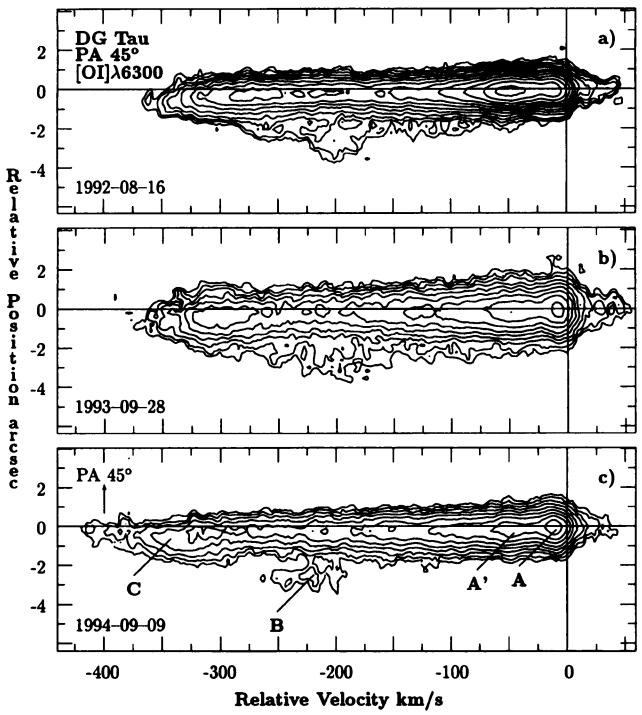

Figure 4. Time series from 1992 to 1994 of the PV diagrams of the [OI]λ6300 line in DG Tau. Position angle, contours, velocities and positions as in Fig. 2

even higher densities within 0.5″ from the star significant line quenching of [SII] occurs such that only [OI] is observable. From an analysis of the higher-density region of the HVC (feature C) on the PV diagrams at PA 45° and PA 135° (Figs. 2 and 3) one derives a spatial extent (FWHM) of ∼0.″7 (∼100 AU) and <0.″2 (<30 AU) for the microjet parallel and perpendicular to the outflow direction, respectively. The derived spatial offset of the [OI]λ6300 emission centroid of the HVC increases from 0.″2 to 0.″6 as a function of increasing velocity. A mean velocity of -270 km s^{-1} and a total velocity width of >250 km s^{-1} have been deduced for the microjet from the [OI]λ6300 emission.

The observed "terminal" velocity of the "blue wing" of the [OI]λ6300 line has increased significantly during 1992–1994. This suggests that probably a new mass ejection event has occurred duing that period. Interestingly, the gas in the more recent flow is faster than that in the precursor. This implies that the gas of the new ejection will eventually overtake that of the previous ejection and hence produce internal shocks in the jet flow.

https://doi.org/10.1017/S0074180900061544 Published online by Cambridge University Press

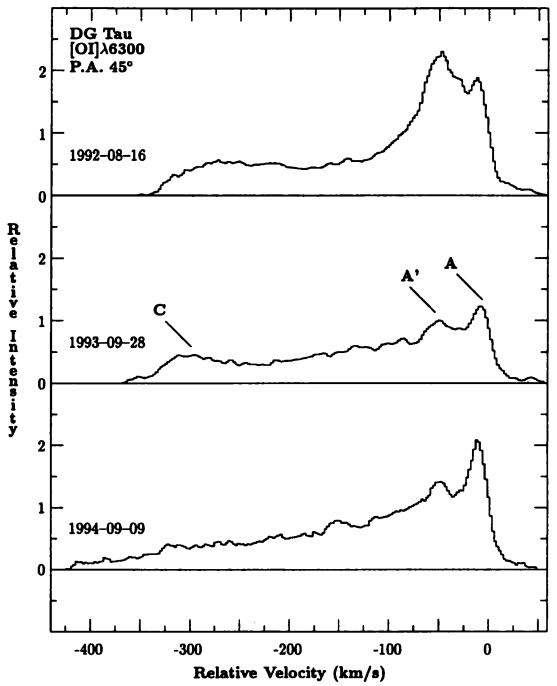

Figure 5. Time series of the [OI]λ6300 line intensity profiles in DG Tau (see Fig. 4)

3.2.4. *The low-velocity gas component (LVC)*

The LVC, represented by feature A' (see Figs. 2–4), is detected in [OI]λ6300 and [SII]λ6731. It is not detected in [OI]λ5577 and [NII]λ6583. The latter indicates a lower excitation in the LVC compared to the HVC. The derived electron density of the LVC is comparable to that of the HVC, but significantly lower than that of the NRVC. A centroid velocity of -43 km s^{-1} and velocity width (FWHM) of 39 km s^{-1} have been measured. The emission centroid of the LVC is offset from the stellar position by 0.″11 (15 AU) and 0.″25 (35 AU) in [OI]λ6300 and [SII]λ6731, respectively. The spatial width (corrected FWHM) of the LVC deduced for [OI]λ6300 is ∼0.″3 (∼40 AU) in both directions, parallel and perpendicular to the flow. The velocity profile of the LVC is highly asymmetric presenting an extended blueshifted wing. The spatial offset of the emission in that wing becomes progressively larger if one proceeds to larger (negative) velocities. Remarkably, the high-velocity wing of the LVC extends into the domain of the HVC (feature B) and is confused by the emission of the HVC such that no clear distinction can be made between the LVC and HVC in that velocity range. This indicates that the HVC and LVC may be physically related to each other in the sense

https://doi.org/10.1017/S0074180900061544 Published online by Cambridge University Press

that a transition zone exists between the associated two gas components. Because of these findings we suggest that the LVC is attributed to a slower gas in the environment of the jet which is entrained by the faster jet gas. This interpretation is well compatible with the different spatio-kinematic properties and excitation conditions deduced for the LVC and HVC.

3.2.5. *The near-rest-velocity gas component (NRVC)*
The NRVC, represented by feature A (Fig. 2–5), is detected in [OI]λ6300 and [OI]λ5577, but not detected in [NII]λ6583 and [SII]λ6731, indicating both a lower excitation and a higher density compared to the HVC and LVC. Remarkably, the [OI]λ6300 profile, peaking at -15 km s^{-1}, shows an extended redshifted wing reaching up to $\sim +50$ km s^{-1}. The offset from the stellar position deduced for the emission centroid of the NRVC is $0.''11$ (15 AU) and $\leq 0.''05$ ($\leq$7 AU) for [OI]λ6300 and [OI]λ5577, respectively. The spatial extent (corrected FWHM) derived for [OI]λ6300 is $\sim 0.''3 \times 0.''4$ ($\sim$ 42 AU $\times$ 56 AU), parallel and perpendicular to the flow, respectively. These findings indicate that the NRVC represents a compact region of an intrinsically slow, high-density gas concentrated in the immediate vicinity of the outflow source. This result lends strong support to the model of Kwan & Tademaru (1988; 1995) in which the NRVC is attributed to a slow disk wind and/or disk corona. The redshifted line wing is probably due to rotation as expected for a line forming region corotating with the disk.

References

Appenzeller, I., Jankovics, I. & Östreicher, R. 1984, A&A, 141, 108
Böhm, K.-H. & Solf, J. 1994, ApJ, 430, 277
Edwards, S., Cabrit, S., Strom, S.E., Heyer, I., Strom, K.M. & Anderson, E. 1987, ApJ, 321, 473
Eislöffel, J. 1992, Ph.D. thesis, Univ. Heidelberg
Gómez de Castro, A.I. & Pudritz, R.E. 1993, ApJ, 409, 748
Hamann, F. 1994, ApJS, 93, 485
Hartigan, P., Edwards, S. & Ghandour, I. 1995, ApJ, 452, 736
Hartmann, L.W. & Raymond, J.C. 1989, ApJ, 337, 903
Hirth, G.A., Mundt, R. & Solf, J. 1994a, A&A, 285, 929
Hirth, G.A., Mundt, R., Solf, J. & Ray, T.P. 1994b, ApJ, 427, L99
Hirth, G.A., Mundt, R. & Solf, J. 1997, A&A, submitted
Kwan, J. & Tademaru, E. 1988, ApJ, 332, L41
Kwan, J. & Tademaru, E. 1995, ApJ, 454, 382
Mundt, R., Brugel, E.W. & Bührke, T. 1987, ApJ, 319, 275
Mundt, R. & Fried, J. 1983, ApJ, 274, L83
Ouyed, R. & Pudritz, R.E. 1993, ApJ, 419, 255
Solf, J. 1989, in: ESO Conf. Proc. 33, Low Mass Star Formation and Pre-Main Sequence Objects, Ed. B. Reipurth, (Garching b. München: ESO), p. 399
Solf, J. 1994, in: ASP Conf. Ser. 57, Stellar and Circumstellar Astrophysics, ed. G. Wallerstein & A. Noriega-Crespo (San Francisco: ASP), p. 399
Solf, J. & Böhm, K.-H. 1993, ApJ, 410, L31